scientific reports

Check for updates

OPEN

Marangoni convection in dissipative flow of nanofluid through porous space

Ikram Ullah[1], Mohammad Mahtab Alam[2], Muhammad Irfan Shah[3] & Wajaree Weera[4]✉

In various machinery engines, the engine oil is utilized as a lubricant. Heat transportation rate and to saving the energy dissipated due to higher temperature are the basic goals of all thermal systems. Thus, current work is mainly focused to develop a model for the Marangoni flow of nanofluids (NFs) with viscous dissipation. The considered NFs are made of nanoparticles (NPs) i.e. $CoCr_{20}W_{15}N$ and base fluid (BF) as Engine Oil (EO). Darcy Forchheimer (DF) law which leads to porous medium is implemented in the model to investigate the variation of velocity and temperature. The governing flow expressions are simplified through similarity variables. The obtained expressions are solved numerically via an effective technique known as the NDSolve algorithm. The consequences of pertinent variables on temperature, velocity and Nusselt number are designed through tables and graphs. The obtained results reveal that velocity rises for higher Marangoni number, Darcy Forchheimer (DF) parameter whereas it shows decaying behavior against nanoparticles volume fraction.

The addition of nanometer-sized tiny particles in a liquid is term as nanofluid. Oxides, carbides, carbon nanotubes, and metals are used as nanoparticles in base fluids like water, methanol, blood, oil, and ethylene glycol[1]. The structure of nanoparticles used in the regular liquid is limited to dimensions of (1–100 nm). The physical features of such fluids are attributed to tiny structures and are distinct from those observed in large farmworker. The characteristic physical scaling lengths of fluids have a strong correlation with the dimensions of nanostructures, especially those that have dimensions in micrometer. The diameters of nanostructures, especially those with micrometer dimensions, have a strong association with the physical scaling lengths of fluids. Nanofluids in heat transmission are used in fuel cells microelectronics, pharmaceutical procedures in engine like hybrid-powered, engine cooling/vehicle thermal management, home freezers, chillers, and boilers to name a few. They have the highest thermal potential than the base fluid. Understanding of the characteristic of nanofluids is considered to be evaluative in determining their viability for thermal transport applications. Nanofluids also have typical acoustical behavior, such as extra shear-wave reconversion of an incident compressional wave in the ultrasonic region which becomes more powerful as concentration enhances. In computational fluid dynamics simulations, nanofluids can be regarded as single-phase fluids, however, most current academic studies assume that nanofluids are two-phase fluids with the physical properties of the nanofluids being a function of both species attributes and concentrations. As an alternative, a two-component model is utilized to simulate nanofluids. The nanoparticles solid-like structure created along the contact line via diffusion aids in the spread of a nanofluid droplet, resulting in disjoining pressure near the contact line. Such enrichment is not conceivable for small droplets with sizes on the nanoscale due to the wetting time scale being substantially shorter than the diffusion time scale. A number of materials like water, oils, glycols, etc. have been utilized as regular liquid. But stabilization is difficult, however continuing research demonstrates that it is possible. Nanofluids have so far been made with metallic particles, oxide particles, and carbon nanoparticles. Researchers have created an ultrasensitive optical sensor based on nanofluids that changes color when exposed to harmful cautions at extremely low concentrations. The sensor can detect trace amounts of cautions in both industrial and environmental samples. Cautions levels in environmental and industrial samples are now measured using expensive, time-consuming, and complicated technologies. Magnetized nanoparticles made up of nano-droplets containing magnetic granules added in water are used to power the sensor. The nanofluid is illuminated in a magnetic field by a light source, and the nanofluid's

[1]Department of Natural Sciences and Humanities, University of Engineering and Technology, Mardan 23200, Pakistan. [2]Department of Basic Medical Sciences, College of Applied Medical Science, King Khalid University, Abha 61421, Saudi Arabia. [3]Department of Sciences and Humanities, National University of Computer and Emerging Sciences, Islamabad 44000, Pakistan. [4]Department of Mathematics, Faculty of Science, Khon Kaen University, Khon Kaen 40002, Thailand. ✉email: wajawe@kku.ac.th

RETRACTED ARTICLE

colour changes with the concentration of cautions. This color switch happens in a split second. Defects in ferromagnetic components can also be detected and imaged using response stimulus nanofluids. Magnet-dependent nanobeads with a size of 80–150 nm produce ordered structures with regular antiparticle spacing in the range of 100 nm, developing in high visible light diffraction. Nano lubricants are another term for suspensions made up of nanoparticles. Different oil utilized for machine and engine lubrication is primarily utilized to make them. Nano lubricants have previously been made from a variety of materials, like oxides, metals, and carbon allotropes. Despite the fact that MoS2, graphene, Cu, etc. base materials have been widely researched, a basic knowledge of the underlying mechanics is still required. Graphene operate as third-body lubricants, transforming into small ball bearings that minimize friction between two touching surfaces. If there is enough impact of the aforementioned particles towards the contract surface, this mechanism works well. As the crumbling process drives out the 3rd body lubricants, the positive effects are lessened. Changing the lubricant, on the other hand, will cancel out the influence of the nano lubricants evacuating through oil. According to numerous studies, nanoparticles can be employed to improve the recovery of crude oil. Comparatively, using nanofluids instead of conventional fluids increases the heat transfer rate in different applications[2–4]. It is very essential to understand the thermal conductivity, viscosity, and specific heat of nanoparticles so that the nanofluids, comprising of these nanoparticles, may be utilized in different applications. Choi et al.[5] studied that in the increasing of heat initial limitation of energy is the Low thermal conductivity. Nanofluids are used in industry. Eastman et al.[6] when contrasted to the liquids without diffused nanocrystalline nanoparticles, then they have extremely high thermal conductivities. Mahanthesh et al.[7] computed the numerical solution of magnetized nanofluid flow through a non-linear stretching surface. Ullah et al.[8] visualized the magnetized nanomaterial flow through rotating surfaces with the application of heat sources. They concluded that temperature enhances thermophoretic and heat source parameters. Ali et al.[9] analyzed the nanomaterials 3D flow through a stretching sheet. They used the FMD technique for the solution of the assumed problem. Nadeem et al.[10] analyzed the viscous nanomaterials flow over a curved surface under the application of the magnetic effect. Ali et al.[11] studied the $Go-MoS_2$ nanoparticles conveying engine oil flow through a vertical oscillating cylinder. They found that $Go-MoS_2$/engine oil-based hybrid nonmaterials boost up the heat transfer rate up to 27%. Mohammadein et al.[12] theoretically disclosed the consequences of radiated nanoparticles conveying water on the stretched surfaces with injection/suction. Their outcomes manifest that the temperature diminishes with higher injection/suction and radiation parameter. Alghahdi et al.[13] perform an experimental analysis of hybrid $WO_3-MWCNTs$/engine oil-based nanomaterials. They explored that the nanomaterial viscosity decays with rise in temperature while it grows up with the addition of nanoparticles. Asadi et al.[14] showed that the support vector regression (SVR) method is very effective for thermo-physical properties. According to this method, if there is rise in temperature then the thermal conductivity will be increased. An enhancement in solid concentration is due to an increase in thermal conductivity. Murad et al.[15] numerically discussed the transformation of heat. Ullah et al.[16] analyzed the entropy for the two types of CNTs i.e. multi-walled and single-walled. Ullah et al.[17] studied the entropy analysis in flow of nanoparticles through Darcy Forchheimer space. Mahanthesh et al.[18] studied the importance of viscous and Joule heating on hybrid nanofluid (MoS_2-Ag) flow on the wedge. Mahanthesh and Mackolil[19] explored the approximations of quadratic thermal radiation and quadratic Boussinesq on nanofluid flow by vertical plate. They used the finite difference method for the solutions of the non-linear differential problem. Dogonchi et al.[20] investigated the natural convection of magnetized nanomaterials flowing an enclosure that is considered porous.

Due to the high surface tension of energy gradient and solute gradient the Marangoni convection occurs. Marangoni convection occurs in a vacuum, and its significance may occur in substrate action, radiations of energy and growth of the crystal, increasing of silicon, measurement of height between points, and other developed uses. Akbar[22] analyzed the nanofluids boundary layer Marangoni convection flow to study the effect of heat transportation. He examined the effect of natural convection on arranging unsteady fluid flow with a vertical heated plate in a porous medium. Wahid et al.[23] explored the Marangoni flow of hybrid nanomaterials over a rotating disk implanted in a porous space. Hossain et al.[24] analyzed the transient combined convective flow of dusty liquid due to small fluctuation in surface and ambient temperature by wedge placed vertically. Sandeep et al.[25] established the Maxwell dusty liquid model under the action of solar radiation, variable surface tension, surface suction, and temperature-dependent viscosity. They discussed the physical characteristics of several parameters against various distributions. AlQdah et al.[26] analyzed the dust particles Marangoni convection of Maxwell nanomaterials with varying viscosity and surface tension. Pearson et al.[27] examined the importance of Marangoni flow and determined the cellular movement driven by surface tension. Chamkha et al.[28] studied the Marangoni combined convection flow driven by pressure gradient and surface tension effect. Zueco and Beg[29] extend the work of Lin et al.[30] to examine Marangoni hydrodynamic flow in hollow pseudo-plastic nanomaterials and incorporate the quadratic form of surface tension into account. Lin et al.[31] used power-law nanofluids to investigate thermal Marangoni convection exposed to Fourier's law with a modified version using viscous fluid as a testing fluid. Mahabaleshwar et al.[32] explored Marangoni radiated convection on thermo-solutal flow via a porous system. Many investigations on Marangoni convection have been conducted, with many intriguing results published in Zheng and Zhang's book[33]. Crystal formation, combustion reactions, heat exchangers, computer discs, rotating machines, and many more applications use operating fluids flowing on a disc. Few other significant attempts in this regard can be consulted through[34–37].

The $CoCr_{20}W_{15}Ni$ alloy is used as the basis of material design for superalloys[38]. The detrimental topologically close packed phases of $CoCr_{20}W_{15}Ni$ system has large ternary extensions which is a useful feature of providing a reliable description of the (TCP) phase boundaries. Stents used in cardiovascular diseases are mostly metallic having large size and should be of small size. No significant change in the microstructure of these stents has been achieved. The thermomechanical treatment of $CoCr_{20}W_{15}Ni$ alloys changes their microstructural properties like grain growth, precipitate formation, and phase transformation which effect the mechanical properties and corrosion resistance[39]. Because of its excellent mechanical properties and corrosion resistance, $CoCr_{20}W_{15}Ni$

RETRACTED ARTICLE

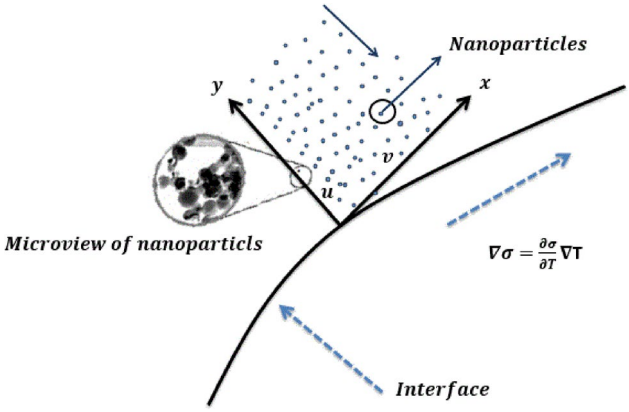

Figure 1. The modeled flow problem geometric configuration.

alloys are used in manufacturing expandable stents which are utilized in cardiovascular diseases[39]. However, the relationship between the microstructure and mechanical properties of $CoCr_{20}W_{15}Ni$ alloy tubes has not been reported yet.

In view of the above literature, there is no study available on EO based $CoCr_{20}W_{15}Ni$ nanoparticles. Therefore, objective here is to discuss the Marangoni flow of cobalt chromium wolfram (tungsten) nickel ($CoCr_{20}W_{15}Ni$) alloy NPs conveying EO through porous space. The novelty of current research is:

- To explore the thermal applications of $CoCr_{20}W_{15}Ni$ alloy suspended in the EO base fluid.
- Darcy Forchheimer (DF) concept is used to visualize the variations in NF temperature and velocity.
- Dissipation of energy is considered for further investigation of heat transfer.
- Surface tension varying linearly with temperature is considered.
- To investigate the rate of heat transfer against different parameters.

The modeled system is dimensionless with pertinent variables. Obtained systems of ODE are approximated with the help of the NDSolve technique. The computed outcomes are depicted via tables and graphs. Comparative analyses of EO and nanofluid are provided and elaborated.

Mathematical modeling

Our intention here is to model the Marangoni convective flow of NFs through infinite disk. Nanofluids are prepared by the addition of $CoCr_{20}W_{15}Ni$ NPs in Engine oil. Engine oil is treated as a base liquid. The Darcy Forchheimer concept for the porous space is utilized. Incompressible 2D and steady flow is addressed (see Fig. 1). Dissipation phenomena is considered in modeling of energy equation. It is further assumed that NP possesses uniform size and shape and is dispersed uniformly in the EO. In light of these considerations, the governing expressions take the form[40,41]:

$$\frac{\partial u}{\partial x} + \frac{\partial v}{\partial y} = 0, \tag{1}$$

$$\rho_{nf}\left(u\frac{\partial u}{\partial x} + v\frac{\partial u}{\partial y}\right) = \mu_{nf}\frac{\partial^2 u}{\partial y^2} + \frac{\mu_{nf}}{k_p}u - Fu^2, \tag{2}$$

where ρ_{nf} stands for the density of nanoliquid, $(u,\ v)$ manifests the velocity components in (xy) directions, μ_{nf} represents dynamic viscosity of NF and k_p shows the permeability of porous medium. Considering surface tension varying with temperature linearly i.e.[31,32]:

$$\left.\begin{aligned} \sigma &= \sigma_0[1 - \gamma_T(T - T_\infty)], \\ \gamma_T &= -\tfrac{1}{\sigma_0}\tfrac{\partial\sigma}{\partial T}\big|_{T=T_\infty}, \end{aligned}\right\} \tag{3}$$

where σ_0 is positive constant and γ_T denotes the surface tension coefficient. The relevant conditions are[10]:

$$\left.\begin{aligned} \mu_{nf}\left.\tfrac{\partial u}{\partial y}\right|_{y=0} &= \left.\tfrac{\partial\sigma}{\partial y}\right|_{y=0} = \left.\tfrac{\partial\sigma}{\partial T}\tfrac{\partial T}{\partial y}\right|_{y=0}, \quad u|_{y=0} = 0, \\ u|_{y\to\infty} &= 0. \end{aligned}\right\} \tag{4}$$

Energy expression. The expression for energy accounting viscous dissipation is

RETRACTED ARTICLE

$$(\rho c_p)_{nf}\left(u\frac{\partial T}{\partial x}+v\frac{\partial T}{\partial y}\right)=k_{nf}\left(\frac{\partial^2 T}{\partial y^2}\right)+\mu_{nf}\left(\frac{\partial u}{\partial y}\right)^2 \tag{5}$$

with

$$T|_{y=0}=T_\infty+TX^2,\ \ T|_{y\to\infty}=T_\infty, \tag{6}$$

where n manifests the exponential index, $(\rho c_p)_{nf}$ the heat capacitance, k_{nf} the thermal conductivity, T stands for temperature, and (T_0,T_∞) the disk and ambient liquid temperature.

Transformations. The transformed variables are

$$\left.\begin{aligned} u=\frac{\nu_f}{L}Xf'(\eta), v=\frac{\nu_f}{L}f(\eta),\\ T_0=T_\infty+T_0X^2\theta(\eta),\ \eta=\frac{y}{L}, X=\frac{x}{L}. \end{aligned}\right\} \tag{7}$$

Upon using Eqs. (7), (1) reduces to identity while other expressions are

$$\frac{A_1}{A_2}f'''+\beta\frac{A_1}{A_2}f'-Frf'^2-f'^2+ff''= \tag{8}$$

$$\frac{A_4}{A_3}\frac{1}{\Pr}\theta''-2f'\theta+f\theta'+\frac{A_1}{A_2}Ecf''= \tag{9}$$

$$\left.\begin{aligned} f(\eta)\big|_{\eta=0}=0,\ f''(\eta)\big|_{\eta=0}=-2M\ A_1,\ \theta(\eta)|_{\eta=0}=1,\\ f'(\eta)\big|_{\eta=\infty}=\ \ \theta(\eta)|_{\eta=\infty}=0, \end{aligned}\right\} \tag{10}$$

where

$$A_1=(1-\phi)^{2.5} \tag{11}$$

$$A_2=\left((1-\phi)+\phi\left(\frac{\rho_s}{\rho_f}\right)\right), \tag{12}$$

$$A_3=\left((1-\phi)+\phi\frac{(\rho c_p)_s}{(\rho c_p)_f}\right), \tag{13}$$

$$A_4=\frac{k_s+(n-1)k_f-(n-1)\phi(k_f-k_s)}{k_s+(n-1)k_f+\phi(k_f-k_s)}. \tag{14}$$

Here β is the Darcy number, Fr be the Forchheimer parameter, ϕ denotes the nanoparticles volume fraction, Ma is the Marangoni number, Ec is the Eckert number, Pr is the Prandtl number. These quantities are

$$\left.\begin{aligned} \beta=\frac{L^2}{k_p},\ Fr=\frac{xc_b}{\sqrt{k_p}},\ \ Ec=\frac{\nu_f^2}{(c_p)T_0L^2},\\ \Pr=\frac{\mu_f(c_p)}{k_f},\ \ \mathrm{Ma}=\frac{T_0\gamma_TL^2}{\mu_f\nu_f}. \end{aligned}\right\} \tag{15}$$

Physical quantity. In dimensional form the Nusselt number (Nu_x) is given by

$$Nu_x=\frac{xq_w}{k_f(T_0-T_\infty)}, \tag{16}$$

where q_w shows the wall heat flux and can be expressed as follows:

$$q_w=-k_{nf}\frac{\partial T}{\partial y}\bigg|_{y=0}. \tag{17}$$

In dimensionless case, we have

$$Nu_x=-\frac{x}{L}\frac{k_{nf}}{k_f}\theta'(0). \tag{18}$$

RETRACTED ARTICLE

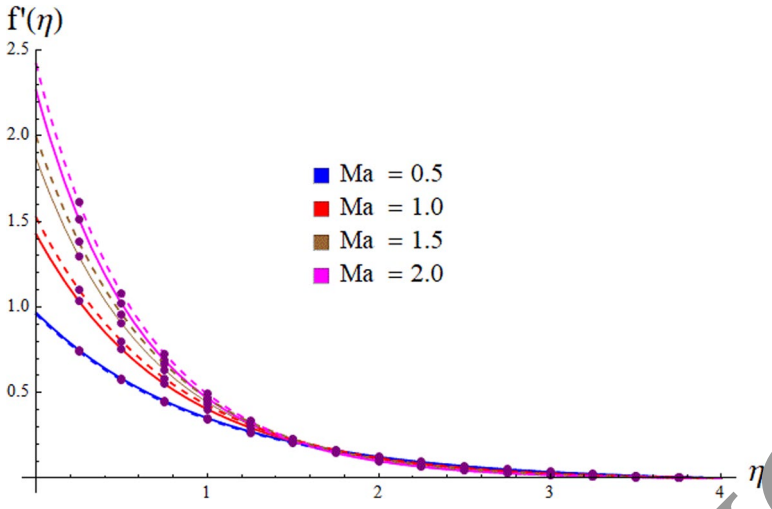

Figure 2. Behavior of velocity $f'(\eta)$ against $Ma = 0.5,1.0,1.5, 2.0$.

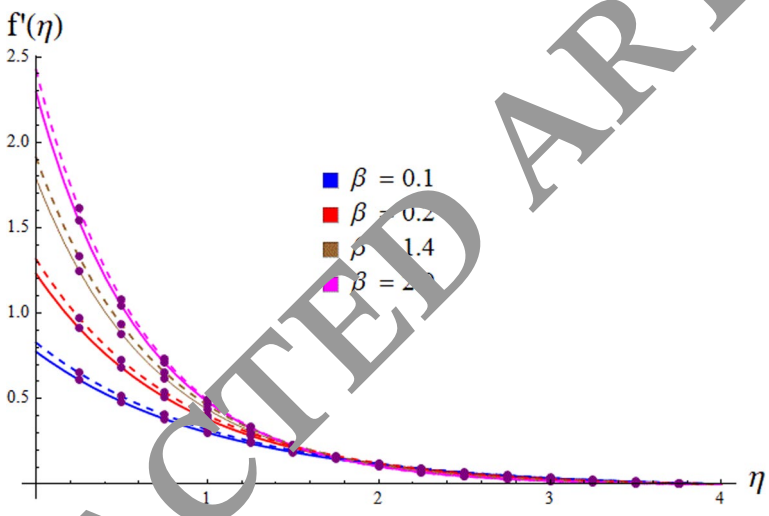

Figure 3. Behavior of velocity $f'(\eta)$ against $\beta = 0.1, 0.2,1.4, 2.0$.

Discussion on outcomes

The reduced Eqs. (8)–(12) has been tackled numerically through the implementation of the NDsolve scheme. Simulations of the nonlinear systems have been executed by employing computer software Mathematica. The main persistence of this section is to declare the behavior of pertinent variables on distinct flow fields graphically. For such an aim, we have designed Figs. 2, 3, 4, 5, 6, 7 and 8 and Table 1. The whole investigation is carried out by considering $CoCr_{20}W_{15}Ni$ nanoparticles in carrier liquid engine oil (EO). Furthermore, the dashed and solid lines depict the NFs and base fluid respectively. The physical properties of nanoparticles and (EO) and their relations for base and nano fluids (NFs) are presented in Tables 2 and 3 respectively. An enhancement in *Ma* escalates the nanomaterials velocity $f'(\eta)$ as explained in Fig. 2. The physical reason behind this behavior is the surface tension caused by thermal gradient. The characteristic of Darcy number β on $f'(\eta)$ is disclosed in Fig. 3. Velocity $f'(\eta)$ becomes low for longer estimations of β. Variation in $f'(\eta)$ against Forchheimer parameter is portrayed in Fig. 4. It is obvious from the figure that $f'(\eta)$ decays for upshot values of *Fr*. In view of physical application, an increment in *Fr* consequently rises internal force and thus $f'(\eta)$ decays. Figure 5 illustrates the impact of ϕ on velocity $f'(\eta)$. It is noted that fluid velocity decays when ϕ enhances. In fact, the transportation of energy in metallic-type materials is faster when compared with dense materials. That is the reason of decaying NFs velocity against higher volume fractions. The change in thermal field $\theta(\eta)$ against *Ec* is designed in Fig. 6. It is observed that, the upshot in *Ec* greatly grows up the nanomatrials temperature. An increase in *Ec*, the mechanical energy of the nonmaterial is converted into thermal energy because of molecules friction. Thus NFs temperature $\theta(\eta)$ increment is observed. Figure 7 gives the behavior of Forchheimer parameter *Fr* on temperature $\theta(\eta)$. Here NFs temperature is enhanced by conceding large values of *Fr*. Physically, larger estimations of Forchheimer parameter boosts up the internal force therefore, NFs temperature $\theta(\eta)$ rises. Impact of ϕ on NFs temperature $\theta(\eta)$ is shown

RETRACTED ARTICLE

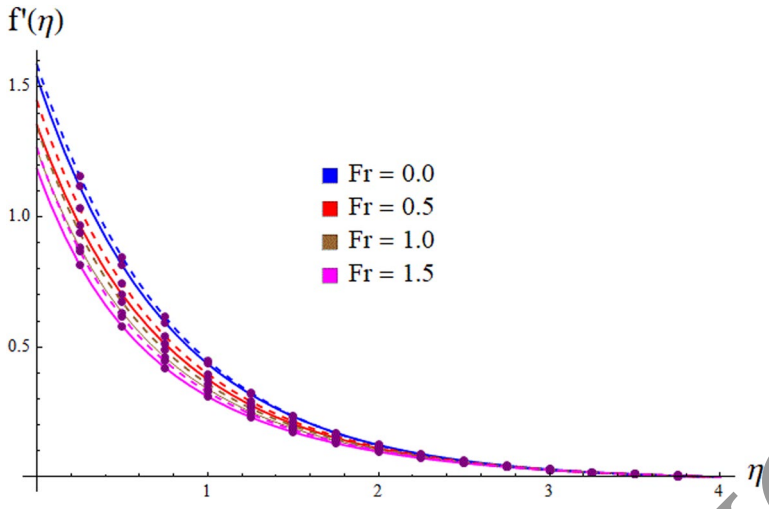

Figure 4. Behavior of velocity $f'(\eta)$ against Fr = 0.0, 0.5,1.0,1.5.

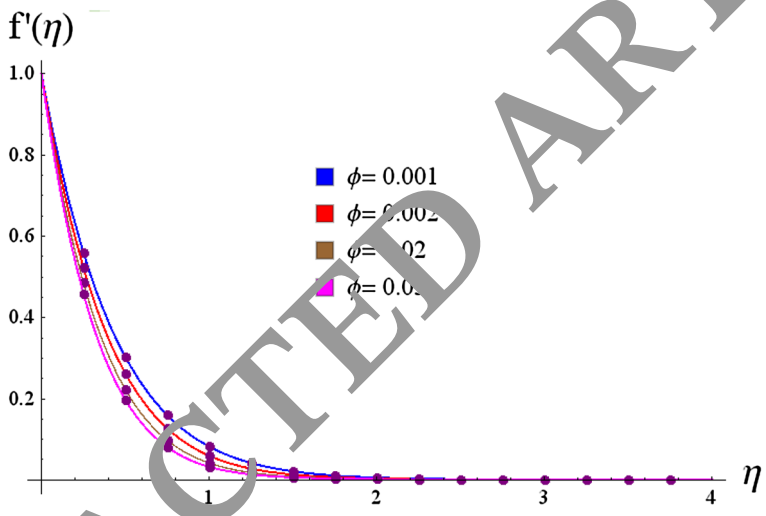

Figure 5. Behavior of velocity $f'(\eta)$ against ϕ = 0.001, 0.002, 0.02, 0.03.

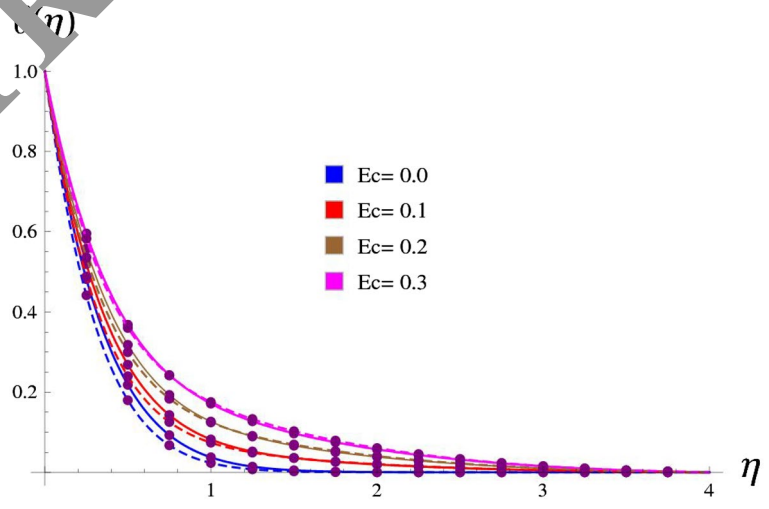

Figure 6. Behavior of temperature $\theta(\eta)$ against Ec = 0.0, 0.1, 0.3, 0.4.

RETRACTED ARTICLE

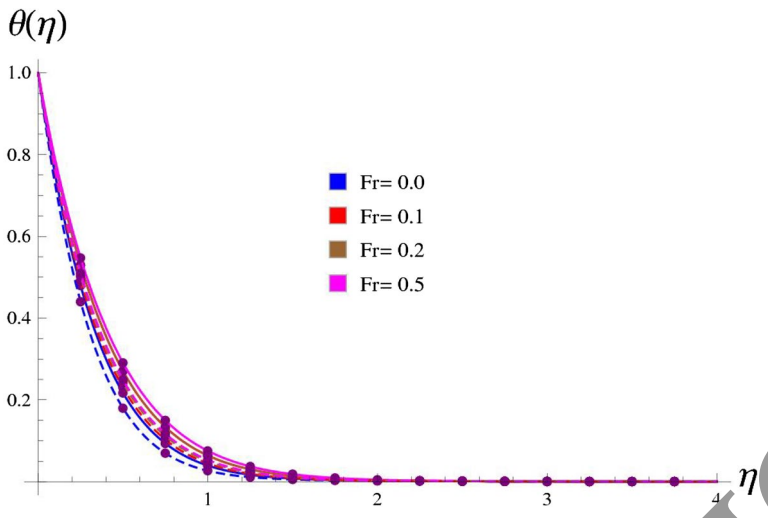

Figure 7. Behavior of temperature $\theta(\eta)$ against Fr = 0.0, 0.1, 0.2, 0.5.

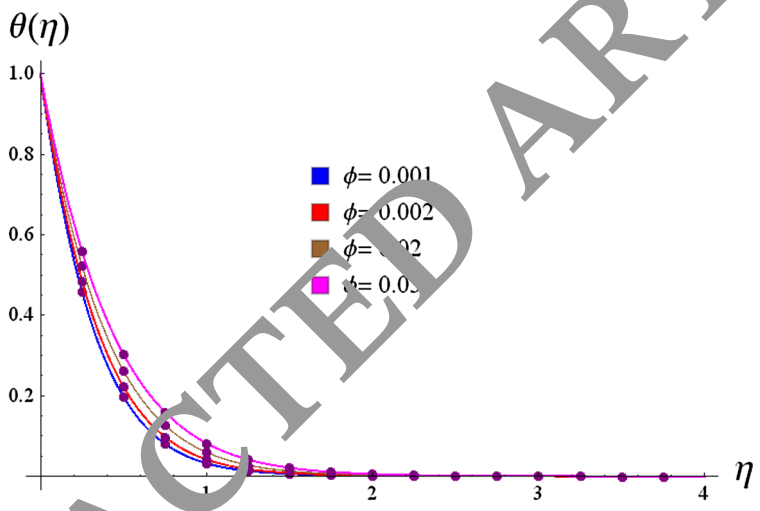

Figure 8. Behavior of temperature $\theta(\eta)$ against ϕ = 0.001, 0.002, 0.02, 0.03.

in Fig. 8. It is acquainted that NFs temperature rises with increasing NPs volume fraction ϕ. In fact, addition of nano-particle volume fraction produces extra heat and this definitely causes improvement in NFs $\theta(\eta)$ and its layer thickness. Table 1 witnesses the computational outcomes of Nusselt number against various parameters i.e. Ec,Ma, ϕ and Fr. It is noted that heat transport rate enhances via ϕ and Ma, where as an opposite trend is seen for Fr and Ec.

Conclusions

The Marangoni flow of NFs containing $CoCr_{20}W_{15}Ni$ and regular liquid engine oil (EO) via porous space is explored. Consequences of Darcy- Forchheimer law are considered. Transformations help to convert the PDEs to ODEs and then solved numerically via ND Solve technique. Key points are as follows:

- Velocity of NFs decays for Ma, β and Fr.
- An enhancement in NPs volume fraction ϕ upsurges the velocity while decays the NFs temperature.
- Enhancement features of E_c and Fr for temperature are observed.
- Reverse trend for E_c and Fr is noted on Nusselt number.
- Rate of heat transportation is evaluated for larger Ma, and ϕ while it diminishes for Fr and E_c.

Furthermore, one may consider the production of entropy, hybrid and ternary hybrid NFs containing different base fluid and NPs, Lorentz force effect etc. as a future work.

RETRACTED ARTICLE

Ec	*Fr*	ϕ	*Ma*	$-\theta'(0)$
0.0	0.1	0.03	0.2	3.110174036118505
0.1				3.085194622900241
0.3				3.035235795678353
0.1	0.0	0.03	0.2	3.1365427002334942
	0.3			2.993026941074681
	0.6			2.875673003228666
0.1	0.1	0.0	0.2	3.0706147987633883
		0.3		3.0851946201806277
		0.8		3.080505675232005
0.1	0.1	0.03	0.0	0.27853759311504883
			0.5	3.86854014981341
			1.0	3.739282989417406

Table 1. Computational outcomes of nusselt number for *Ec*, *Fr*, ϕ and *Ma*.

Constituents	ρ (kg/m^3)	c_p (J/kgK)	k (W/mk)
$CoCr_{20}W_{15}Ni$	9.60	400.0	1
Engine oil	884	1910	0.144

Table 2. Thermal and physical characteristics of $CoCr_{20}W_{15}Ni$ nanoparticles and engine oil[33,34].

Properties	Nanofluid
Density	$\rho_{nf} = \rho_f\left((1-\phi) + \phi\frac{\rho_s}{\rho_f}\right)$
Viscosity	$\mu_{nf} = \frac{\mu_f}{(1-\phi)^{2.5}}$
Heat capacity	$(\rho c_p)_{nf} = (\rho c_p)_f\left((1-\phi) + \phi\frac{(\rho c_p)_s}{(\rho c_p)_f}\right)$
Thermal conductivity	$\frac{k_{nf}}{k_f} = \frac{k_s+(n-1)k_f-(n-1)\phi(k_f-k_s)}{k_s+(n-1)k_f+\phi(k_f-k_s)}$

Table 3. Thermo-physical features of nanofluid ($CoCr_{20}W_{15}Ni$) and engine oil (EO).

Data availability

All the data is given within the manuscript.

Received: 2 June 2022; Accepted: 1 March 2023
Published online: 18 April 2023

References

1. Ullah, I., Hayat, T., Alsaedi, A. & Fardoun, H. M. Numerical treatment of melting heat transfer and entropy generation in stagnation point flow of hybrid nanomaterials (SWCNT-MWCNT/engine oil). *Mod. Phys. Lett. B* **35**(06), 2150102 (2021).
2. Susrutha, B., Ram, S. & Tyagi, A. K. Effects of gold nanoparticles on rheology of nanofluids containing poly (vinylidene fluoride) molecules. *J. Nanofluids* **1**(2), 120–127 (2012).
3. Phule, A. D., Ram, S. & Tyagi, A. K. Anchoring silver with poly (vinylidene fluoride) molecules in model flocculates and its effects on rheology in stable nanofluids. *J. Nanofluids* **2**(4), 249–260 (2013).
4. Singh, G. P. & Ram, S. *Magnetic Nanofluids: Synthesis and Applications" in "Nanofluids, Research, Development and Applications* (Nova Publisher, 2013).
5. Choi, S. U. S., Singer, D. A. & Wang, H. P. Developments and applications of non-Newtonian flows. *ASME Fed.* **66**, 99–105 (1995).
6. Eastman, J. A., Choi, U. S., Li, S., Thompson, L. J. & Lee, S. Enhanced thermal conductivity through the development of nanofluids. *MRS Online Proc. Library* **1**, 457 (1996).
7. Mahanthesh, B., Gireesha, B. J., Gorla, R. R., Abbasi, F. M. & Shehzad, S. A. Numerical solutions for magnetohydrodynamic flow of nanofluid over a bidirectional non-linear stretching surface with prescribed surface heat flux boundary. *J. Magn. Magn. Mater.* **417**, 189–196 (2016).
8. Ullah, I., Alghamdi, M., Xia, W. F., Shah, S. I. & Khan, H. Activation energy effect on the magnetized-nanofluid flow in a rotating system considering the exponential heat source. *Int. Commun. Heat Mass Transf.* **128**, 105578 (2021).
9. Ali, B., Thumma, T., Habib, D. & Riaz, S. Finite element analysis on transient MHD 3D rotating flow of Maxwell and tangent hyperbolic nanofluid past a bidirectional stretching sheet with Cattaneo Christov heat flux model. *Therm. Sci. Eng. Progress* **28**, 101089 (2021).
10. Nadeem, S., Khan, M. R. & Khan, A. U. MHD stagnation point flow of viscous nanofluid over a curved surface. *Phys. Scr.* **94**(11), 115207 (2019).

RETRACTED ARTICLE

11. Arif, M., Kumam, P., Khan, D. & Watthayu, W. Thermal performance of GO-MoS2/engine oil as Maxwell hybrid nanofluid flow with heat transfer in oscillating vertical cylinder. *Case Stud. Therm. Eng.* **27**, 101290 (2021).
12. Mohammadein, S. A., Raslan, K., Abdel-Wahed, M. S. & Abedel-Aal, E. M. KKL-model of MHD CuO-nanofluid flow over a stagnation point stretching sheet with nonlinear thermal radiation and suction/injection. *Results Phys.* **10**, 194–199 (2018).
13. Aghahadi, M. H., Niknejadi, M. & Toghraie, D. An experimental study on the rheological behavior of hybrid Tungsten oxide (WO3)-MWCNTs/engine oil Newtonian nanofluids. *J. Mol. Struct.* **1197**, 497–507 (2019).
14. Asadi, A., Bakhtiyari, A. N. & Alarifi, I. M. Predictability evaluation of support vector regression methods for thermophysical properties, heat transfer performance, and pumping power estimation of MWCNT/ZnO–engine oil hybrid nanofluid. *Eng. Comput.* **37**(4), 3813–3823 (2021).
15. Mourad, A. *et al.* Galerkin finite element analysis of thermal aspects of Fe3O4-MWCNT/water hybrid nanofluid filled in wavy enclosure with uniform magnetic field effect. *Int. Commun. Heat Mass Transf.* **126**, 105461 (2021).
16. Ullah, I., Hayat, T., Aziz, A. & Alsaedi, A. Significance of entropy generation and the coriolis force on the three-dimensional non-Darcy flow of ethylene-glycol conveying carbon nanotubes (SWCNTs and MWCNTs). *J. Non-Equilib. Thermodyn.* **47**, 61–75 (2021).
17. Ullah, I., Hayat, T. & Alsaedi, A. Optimization of entropy production in flow of hybrid nanomaterials through Darcy–Forchheimer porous space. *J. Therm. Anal. Calorim.* **147**, 5855–5864 (2021).
18. Mahanthesh, B., Shehzad, S. A., Ambreen, T. & Khan, S. U. Significance of Joule heating and viscous heating on heat transport of MoS2–Ag hybrid nanofluid past an isothermal wedge. *J. Therm. Anal. Calorim.* **143**(2), 1221–1229 (2021).
19. Mahanthesh, B. & Mackolil, J. Flow of nanoliquid past a vertical plate with novel quadratic thermal radiation and quadratic Boussinesq approximation: Sensitivity analysis. *Int. Commun. Heat Mass Transfer* **120**, 105040 (2021).
20. Dogonchi, A. S., Seyyedi, S. M., Hashemi-Tilehnoee, M., Chamkha, A. J. & Ganji, D. D. Investigation of natural convection of magnetic nanofluid in an enclosure with a porous medium considering Brownian motion. *Case Stud. Therm. Eng.* **14**, 100502 (2019).
21. Yiantsios, S. G. & Higgins, B. G. Marangoni flows during drying of colloidal films. *Phys. Fluids* **18**(8), 082103 (2006).
22. Akbar, N. S., Nadeem, S., Haq, R. U. & Khan, Z. H. Numerical solutions of magnetohydrodynamic boundary layer flow of tangent hyperbolic fluid towards a stretching sheet. *Indian J. Phys.* **87**(11), 1121–1124 (2013).
23. Wahid, N. S., Arifin, N. M., Khashi'ie, N. S. & Pop, I. Marangoni hybrid nanofluid flow over a permeable infinite disk embedded in a porous medium. *Int. Commun. Heat Mass Transfer* **126**, 105421 (2021).
24. Hossain, M. A., Roy, N. C. & Siddiqa, S. Unsteady mixed convection viscous fluid flow past a vertical wedge due to small fluctuation in free stream and surface temperature. *Appl. Math. Comput.* **299**, 80–92 (2017).
25. Sandeep, N., Sugunamma, V. & Mohankrishna, P. Effects of radiation on an unsteady natural convective flow of a EG-Nimonic 80a nanofluid past an infinite vertical plate. *Adv. Phys. Theor. Appl.* **23**, 43 (2013).
26. AlQdah, K. S., Khan, N. M., Bacha, H. B., Chung, J. D. & Siddiqui, A. A. Marangoni convection of dust particles in the boundary layer of Maxwell nanofluids with varying surface tension and viscosity. *Coatings* **11**(9), 1072 (2021).
27. Pearson, J. R. A. On convection cells induced by surface tension. *J. Fluid Mech.* **4**(5), 489–500 (1958).
28. Chamkha, A. J., Pop, I. & Takhar, H. S. Marangoni mixed convection boundary layer flow. *Meccanica* **41**(2), 219–232 (2006).
29. Zueco, J. & Bég, O. A. Network numerical simulation of hydromagnetic Marangoni mixed convection boundary layers. *Chem. Eng. Commun.* **198**(4), 552–571 (2010).
30. Lin, Y., Zheng, L. & Zhang, X. MHD Marangoni boundary layer flow and heat transfer of pseudo-plastic nanofluids over a porous medium with a modified model. *Microgravity Time-dependent Mater.* **19**(4), 519–536 (2015).
31. Lin, Y. H., Zheng, L. C. & Zhang, X. H. Marangoni convection flow and heat transfer of power law nanofluids driven by temperature gradient with modified Fourier law. *Int. J. Nonlinear Sci. Numer. Simul.* **15**(6), 337–345 (2014).
32. Mahabaleshwar, U. S., Nagaraju, K. T., Vinay Kumar, P. N. & Azese, M. N. Effect of radiation on thermosolutal Marangoni convection in a porous medium with chemical reaction and heat source/sink. *Phys. Fluids* **32**(11), 113602 (2020).
33. Zheng, L. & Zhang, X. *Modeling and Analysis of Modern Fluid Problems* (Academic Press, 2017).
34. Magyari, E. & Chamkha, A. J. Exact analytical solutions for thermosolutal Marangoni convection in the presence of heat and mass generation or consumption. *Heat Mass Transf.* **43**(9), 965–974 (2007).
35. Mahanthesh, B., Gireesha, B. J., Shashikumar, N. S. & Shehzad, S. A. Marangoni convective MHD flow of SWCNT and MWCNT nanoliquids due to a disk with solar radiation and irregular heat source. *Physica E* **94**, 25–30 (2017).
36. Khan, F. & Yang, C. Mathematical analysis of two phase saturated nanofluid influenced by magnetic field gradient. *Inventions* **6**(2), 26 (2021).
37. Khan, M., Sarfraz, M., Ahmed, A., Malik, M. Y. & Alqahtani, A. S. Study of engine-oil based CNT nanofluid flow on a rotating cylinder with viscous dissipation. *Phys. Scr.* **96**(7), 075005 (2021).
38. Wang, F. *et al.* Thermodynamic assessment of the Co–Cr–Ni, Co–Cr–W and Co–Ni–W. *Calphad* **73**, 102252 (2021).
39. Geiser, B. P. Topologically close-packed phase prediction in Ni-based superalloys: Phenomenological structure maps and bond-order theory (2011).
40. Ueki, K. *et al.* Overcoming the strength-ductility trade-off by the combination of static recrystallization and low-temperature heat-treatment in Co–Cr–W–Ni alloy for stent application. *Mater. Sci. Eng. A* **766**, 138400 (2019).
41. Ullah, I. Activation energy with exothermic/endothermic reaction and Coriolis force effects on magnetized nanomaterials flow through Darcy-Forchheimer porous space with variable features. *Waves Rand. Compl. Media* **1**, 1–14 (2022).

RETRACTED ARTICLE

Acknowledgements
The authors are thankful to the Deanship of Scientific Research, King Khalid University, Abha, Saudi Arabia, for financially supporting this work through the General Research Project under Grant No. R.G.P.1/125/43.

Author contributions
Dr. I.U. conceptualized and modeled the paper, M.M.A. contributed to approximating the solution and designed the graphs and tabulated data, W.W.helped in the writing of manuscript and M.I.S. corrected the plotted data and grammatical mistakes.

Competing interests
The authors declare no competing interests.

Additional information
Correspondence and requests for materials should be addressed to W.W.

Reprints and permissions information is available at www.nature.com/reprints.

Publisher's note Springer Nature remains neutral with regard to jurisdictional claims in published maps and institutional affiliations.

Open Access This article is licensed under a Creative Commons Attribution 4.0 International License, which permits use, sharing, adaptation, distribution and reproduction in any medium or format, as long as you give appropriate credit to the original author(s) and the source, provide a link to the Creative Commons licence, and indicate if changes were made. The images or other third party material in this article are included in the article's Creative Commons licence, unless indicated otherwise in a credit line to the material. If material is not included in the article's Creative Commons licence and your intended use is not permitted by statutory regulation or exceeds the permitted use, you will need to obtain permission directly from the copyright holder. To view a copy of this licence, visit http://creativecommons.org/licenses/by/4.0/.

© The Author(s) 2023

RETRACTED ARTICLE